Journal of Applied Polymer Science

Pore morphology control and hydrophilicity of polyacrylonitrile ultrafiltration membranes

Shan Gang Ding, Xi Quan Cheng, Zai Xing Jiang, Yong Ping Bai, Lu Shao

State Key Laboratory of Urban Water Resource and Environment (SKLUWRE), School of Chemical Engineering and Technology, Harbin Institute of Technology, Harbin, People's Republic of China

Shan Gang Ding and Xi Quan Cheng contributed equally to this work.

Correspondence to: L. Shao (E-mail: shaolu@hit.edu.cn) and Z.X. Jiang (E-mail: jiangzaixing@hit.edu.cn)

ABSTRACT: The effects of different solvents (dimethyl formamide: DMF and dimethylsulfoxide: DMSO) on the solubility of polyacrylonitrile (PAN) were investigated by the phase diagrams of H_2O/DMF/PAN and H_2O/DMSO/PAN ternary systems through cloud-point titration method at low polymer concentration. The influences of polymer concentrations and temperatures on the morphologies of PAN ultrafiltration membranes were elucidated. The morphologies of fabricated UF membranes were characterized by scanning electron microscopy (SEM) and atomic force microscope (AFM), and the basic performance of ultrafiltration including pure water flux and rejection of BSA were explored. At 25°C, the pure water flux of ultrafiltration membranes at the lower PAN content (16 wt % PAN in 84 wt % DMSO) reached 213.8 L/m/bar and the rejection of BSA was 100%. Interestingly, the water flux of UF membranes dramatically decreased to 20.6 L/m/bar (20 wt %) and 2.9 L/m/bar (24 wt %) when increasing PAN concentrations in DMSO. On the other hand, the hydrophilicity of membranes can be enhanced by increasing coagulation temperatures and polymer concentrations which were characterized by static contact angle, fitting well with the variation tendency of roughness. Although there are many works concerning on the effects of phase inversion conditions on the performance of PAN UF membranes, to our best knowledge, there is seldom works focusing on investigating the membrane hydrophilicity trend by adjusting phase inversion conditions. To disclose the reason of the enhanced hydrophilicity, the water and glycol contact angles of various membranes were measured and the surface tensions were presented. The results illustrated that the enhanced hydrophilicity of PAN UF membranes fabricated at higher temperatures or higher polymer concentrations was due to the higher polarity on membrane surface. Since the vast majority of ultrafiltration membranes in labs and in industrial scale have been fabricated by immersion phase inversion method, this work can provide a guidance to obtain hydrophilic PAN UF membranes by adjusting the process of phase inversion. © 2015 Wiley Periodicals, Inc. J. Appl. Polym. Sci. **2015**, *132*, 41991.

KEYWORDS: membranes; morphology; properties and characterization; separation techniques

Received 21 September 2014; accepted 15 January 2015
DOI: 10.1002/app.41991

INTRODUCTION

Membrane technology is considered to be one of the most promising high-techs typically applied in the chemical and petrochemical industry, food industry, pharmaceutical industry, and other industrial fields.[1–12] When separating liquid-based mixtures, membrane separations can be typically classified as microfiltration (MF), ultrafiltration (UF), nanofiltration (NF), and reverse osmosis (RO) according to the size of pores. Among the various membrane processes, UF has been considered as the important one because of the broad usages. Currently, most of the industrially used polymeric UF membranes are fabricated by immersion phase inversion method.[13] Therefore, the polymer should be dissolved in polar solvents such as NMP and DMSO to obtain a homogeneous doping solution firstly, consisting of polymer-rich phase and a liquid polymer-lean phase.[14] After casted on a suitable and smooth support, the system is immersed in a non-solvent bath for the phase inversion forming separation membrane. During this process, the membrane is formed from the polymer-rich phase and plenty of pores are produced from the polymer-lean phase.

There are several reports[15–17] studying the influence of the kinetics and thermodynamics of phase separation process on the membrane structure. According to the report by Zhang *et al.*,[18] the rate of solvent exchange was different for water or ethanol as the non-solvent. Kang *et al.*[19] explored the effects of

Shan Gang Ding and Xi Quan Cheng contributed equally to this work.

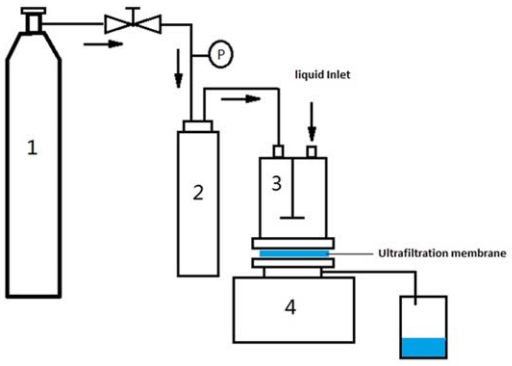

Figure 1. The device for measurement of pure water flux and BSA rejection. [Color figure can be viewed in the online issue, which is available at wileyonlinelibrary.com.]

the molecular weight of polyvinylpyrrolidone (PVP) on the precipitation kinetics during the formation of an asymmetric PAN membrane and the resulting membrane morphology was investigated. The increase of the viscosity of the polymer solution upon the addition of PVP hindered the intrusion of the non-solvent, resulting in a decrease of the phase-separation rate. Tan *et al.*[20] manufactured membranes with the immersion phase inversion method and studied the thermodynamics in phase separation of water/dimethylformamide/polyacrylonitrile ternary systems. They found that the experimental phase diagrams at low polymer concentration fits the theory phase diagram well. Madaeni *et al.*[21] fabricated membrane with phase inversion method, studied the kinetics of phase separating process of water/dimethylsulfoxide/polyethersulfone ternary system, and predicted the membrane microstructure of different polymer concentrations. The sponge-like membranes with relatively dense skin layer were formed at the lower precipitation rate. Chung *et al.*[22–24] made plenty of work on membrane formation and morphology. They have reviewed the limitations of using Flory-Huggins theory to describe the Gibbs free energy for the states of solutions during hollow-fiber formation. They explored the effects of fabrication conditions such as different solvents and different precipitation bath components on membrane morphology. It was found that the membrane morphology strongly depends on the membrane thickness. A critical structure-transition thickness, *Lc*, was observed, indicating the transition of the membrane morphology from a sponge-like to a finger-like structure with an increase in membrane thickness. It has been widely known that the morphology of membrane has the great effect on membrane performance. Thus, it is important to understand kinetics and thermodynamics of membrane-forming systems for obtaining the high-performance membranes.

On the other hand, membrane fouling problem restricts the application and development of PAN UF membrane[25] because of the decaying performance of membrane after fouling. There are lots of methods modifying the hydrophilicity of PAN membrane by introducing special functional groups or polymer layers onto membrane surface.[26–28] Ulbricht *et al.* have carried out a series of study.[29,30] They investigated the heterogeneous surface modifications of PAN membranes with either simultaneous or sequential UV irradiation-initiated graft polymerizations of monomers. The membrane with sufficient degree of modification (grafting) demonstrated the lower contact angles, lower protein adsorption, and almost no fouling to BSA.[30] Although works concerning on enhancing the hydrophilicity of UF membranes have been reported, seldom works focus on exploring the hydrophilicity trend of PAN membrane by adjusting phase inversion conditions.

In this study, the cloud-point curve was determined by the titration method[21,31] for experimentally establishing ternary phase diagrams of H_2O/DMF/PAN and H_2O/DMSO/PAN systems. The solubility of different solvents for PAN can be obtained from the experimental phase diagrams. The experimental phase diagrams of H_2O/DMSO/PAN at higher temperatures were explored and the UF membranes were fabricated by PAN/DMSO at the same temperatures for comparison. Besides, the influence of preparation conditions on the membrane morphology (characterized by scanning electron microscopy and atomic force microscope) and separation performance were investigated in detail. The hydrophilicity of PAN UF membranes was investigated by adjusting the coagulation bath temperature and polymer concentration.

EXPERIMENTAL

Materials

The polyacrylonitrile (PAN) was provided by Qilu Petrochemical Company. Dimethyl formamide (DMF) and dimethylsulfoxide (DMSO) (Tianjin Guangfu Fine Chemical Research Institute) were used as received. Bovine serum albumin (BSA, $M_n = 68{,}000$) was purchased from Beijing Aobo Star Biotechnology Co., Ltd. Deionized water was used in this study.

Membrane Preparation

The immersion phase inversion method was utilized to fabricate the membranes.[32–34] Homogeneous PAN/DMSO solutions (PAN contents of 8 wt %, 12 wt %, 16 wt %, 20 wt %, and 24 wt %) were cast on glass plates with the thickness of 150 μm. The glass plates were immediately immersed in a coagulation bath containing distilled water at 25°C for 24 h. Then, the nascent membranes were moved to a second bath under the same conditions about 24 h. After coagulation was completed, the obtained membranes can be used for basic performance of ultrafiltration. The

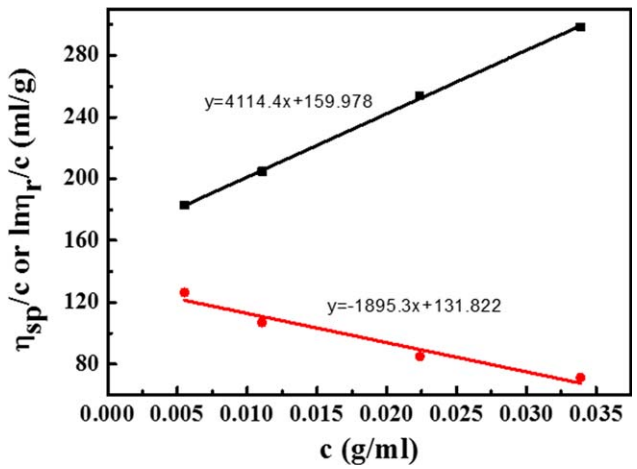

Figure 2. The plots of η_{sp}/c vs. c and $\ln\eta_r/c$ vs. c. [Color figure can be viewed in the online issue, which is available at wileyonlinelibrary.com.]

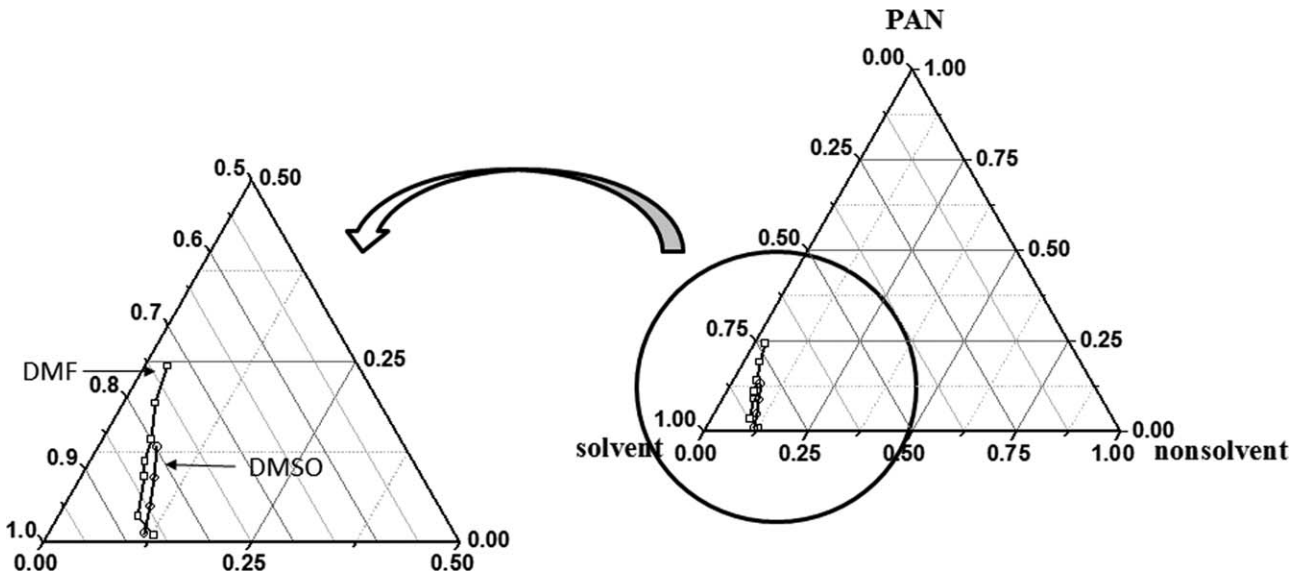

Figure 3. The phase diagram for H_2O/DMF/PAN and H_2O/DMSO/PAN system obtained by experiments at room temperature (the left is the enlarged figure for eye-guidance).

membranes were dried at the room before physicochemical characterization. For investigating the temperature effects, membranes were fabricated at 50°C and 70°C (coagulation bath temperature).

Relative Molecular Weight of PAN

The relative molecular weight of commercial PAN was not provided by the supplier, so the viscosity method was used to determine the relative molecular mass of PAN. Ubbelohde viscometer with the diameter of 0.8–0.9 was used to measure the flowing time of PAN/DMSO dilute solutions at 25°C. In order to assure the accuracy, the measurement at each temperature had been carried out more than three times and the error of flowing time was less than 0.4 s. The viscosity of the polymer solution (η) was generally larger than the viscosity of solvent (η_0), specific viscosity (η_{sp}) can be expressed as the following equation:

$$\eta_{sp} = \frac{\eta - \eta_0}{\eta_0} = \eta_r - 1 \quad (1)$$

where η_r is the relative viscosity. Two straight lines of η_{sp}/c vs. c (c is the solution concentration) and $\ln\eta_r/c$ vs. c can be obtained, respectively.[35] In theory, the two lines can reach one point in the y axis, which was the intrinsic viscosity (η). There was the empirical formula as the following:

$$[\eta] = K \cdot M_\eta^\alpha \quad (2)$$

where K is the proportionality constant for the determined polymer/solvent system at the stipulated temperature, α is a parameter related to the morphology of polymer solution, which is typically between 0.5 to 1.7.

Determination of the Cloud-Point Curve

The cloud-point curve was determined by the titration method.[18,20,36–38] The solutions of PAN in different solvents with various concentrations from 1 wt % to 30 wt % were prepared by mixing of desired amounts of PAN powder and solvents in the sealed conical flasks. These mixtures were stirred with magnetic stirrer until homogeneous solutions achieved. During the titration, distilled water was slowly added into the flask using a syringe with stirring and the polymer solution temperature was controlled at 25°C with a thermostatic H_2O bath. When the turbidity appeared, the addition of water was stopped. If the cloudy solution can be

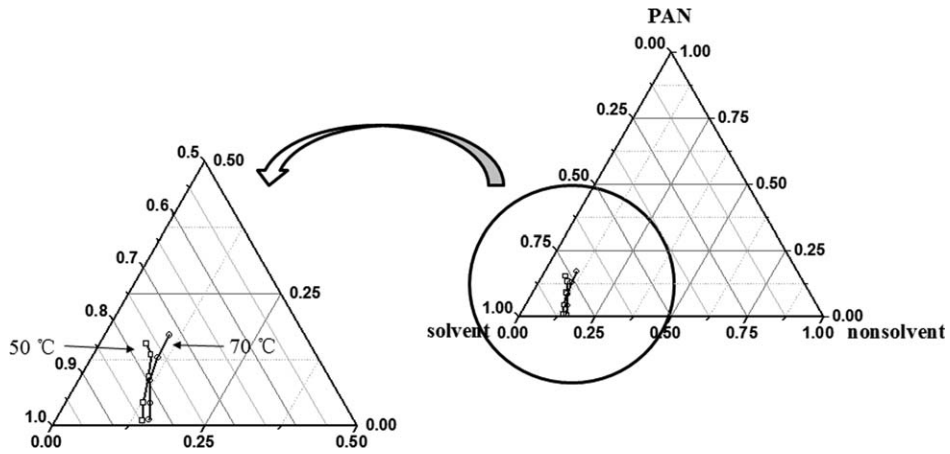

Figure 4. The phase diagram of H_2O/DMSO/PAN system at 50°C and 70°C (The left is the enlarged figure for eye-guidance).

Table I. The Pure Water Flux and BAS Rejection of Different UF Membranes Fabricated by Various Concentrations of PAN in DMSO

	PAN concentrations (wt %)						
	8[a]	12[a]	16	20	24	18[39]	14[40]
Water flux (L/m^{2}h)	-	-	213.8	20.6	2.9	88	42
BSA rejection (%)	-	-	100	100	100	94	90

[a] The mechanical strength of membranes is too low to test.

kept for at least 30 min, this point was considered as the onset of the cloud point. Otherwise, the water was added into the solutions continuously for determination. Then, the phase diagrams were plotted based on the obtained data.

Measurement of Pure Water Flux and BSA Rejection

Pure water flux and BSA rejection of UF membranes were measured by a homemade dead-end filtration system (Figure 1). The distilled water passing through UF membrane under 0.1 MPa in one minute was measured. The pure water flux (F_0) was calculated as the following equation:

$$F_0 = \frac{V}{St} \tag{3}$$

where V is the volume of pure water, S is effective area of membrane, and t is the time of measurement.

The 200 ppm BSA was used for rejection test. Both the feed and permeate solutions were tested by UV-vis spectrometer at 280 nm. The BSA rejection (R) of the membrane was calculated as the following:

$$R = \left(1 - \frac{C_P}{C_f}\right) \times 100\% \tag{4}$$

where C_P is the BSA concentration of filtrate and C_f is the BSA concentration of standard solution.

Morphological Characterizations

The morphology of the fabricated membranes was characterized by a scanning electron microscope (SEM, SEM Quanta 200F, FEI Company). The cross-section morphologies of the membranes were prepared by breaking the membranes in liquid nitrogen to avoid destroying the pore structures of the membranes. AFM machine (Solver P47 Atomic Force Microscopy, Russia) was used to observe the surface morphology of membranes fabricated with different polymer concentration at various temperatures.

Static Contact Angle

Sessile drop method was used to measure the static contact angle of the samples. A contact angle measuring system (G10 Kruss, Germany) was used to measure the static water contact angle of membranes. The membranes were dried in natural conditions and cut into the stipulated size (width of 0.5 cm and length of 5 cm). The cut membranes were stuck on flat glass surface with double side tape and placed on the sample stage. A droplet of water or glycol drops on the membrane surface and was quickly captured by a video camera. Then, the computer fitted calculation and gave the results. The calculation equations were as the following:

$$\gamma_{SL} = \gamma^S + \gamma^L - 2\left(\gamma_S^{\mathrm{d}}\gamma_L^d\right)^{1/2} - 2\left(\gamma_S^P\gamma_L^P\right)^{1/2} \tag{5}$$

where γ^L is interfacial tension, γ^S, γ_S^d, and γ_S^P are polymer interface energy, dispersion component, and polar component,

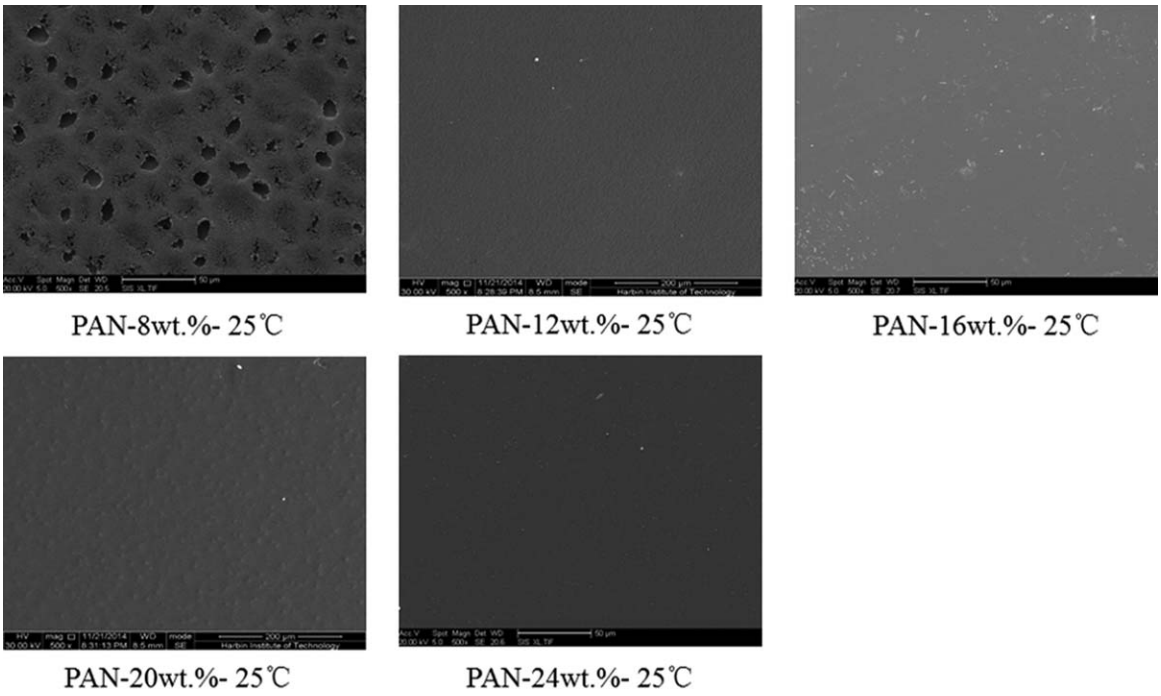

Figure 5. The top surface morphology of membranes prepared from H_2O/DMSO/PAN ternary systems.

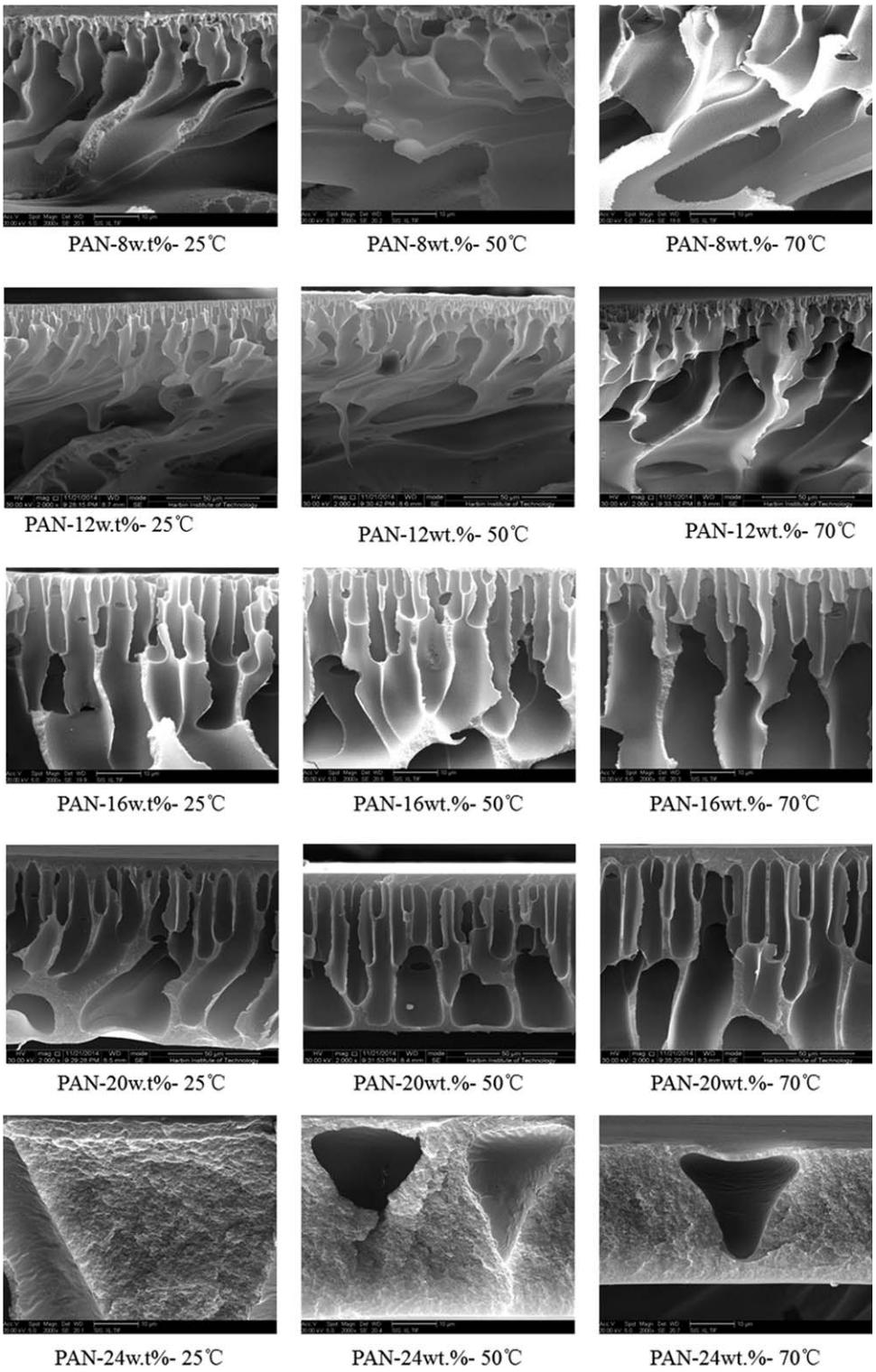

Figure 6. The cross section morphology of all membranes.

respectively. γ^L, γ_L^P, and γ_L^d are liquid interface energy, dispersion component, and polar component respectively. Combining eq. (5) and Young equation, eq. (6) can be deduced:

$$(1+\cos\theta)\gamma^L = 2\left(\gamma_S^d\gamma_L^d\right)^{1/2} + 2\left(\gamma_S^P\gamma_L^P\right)^{1/2} \quad (6)$$

RESULTS AND DISCUSSION

Polymer Relative Molecular Weight

It is well known that the molecular weight of polymer can affect the solubility of polymer in solvent and change the phase diagram. To measure polymer relative molecular weight

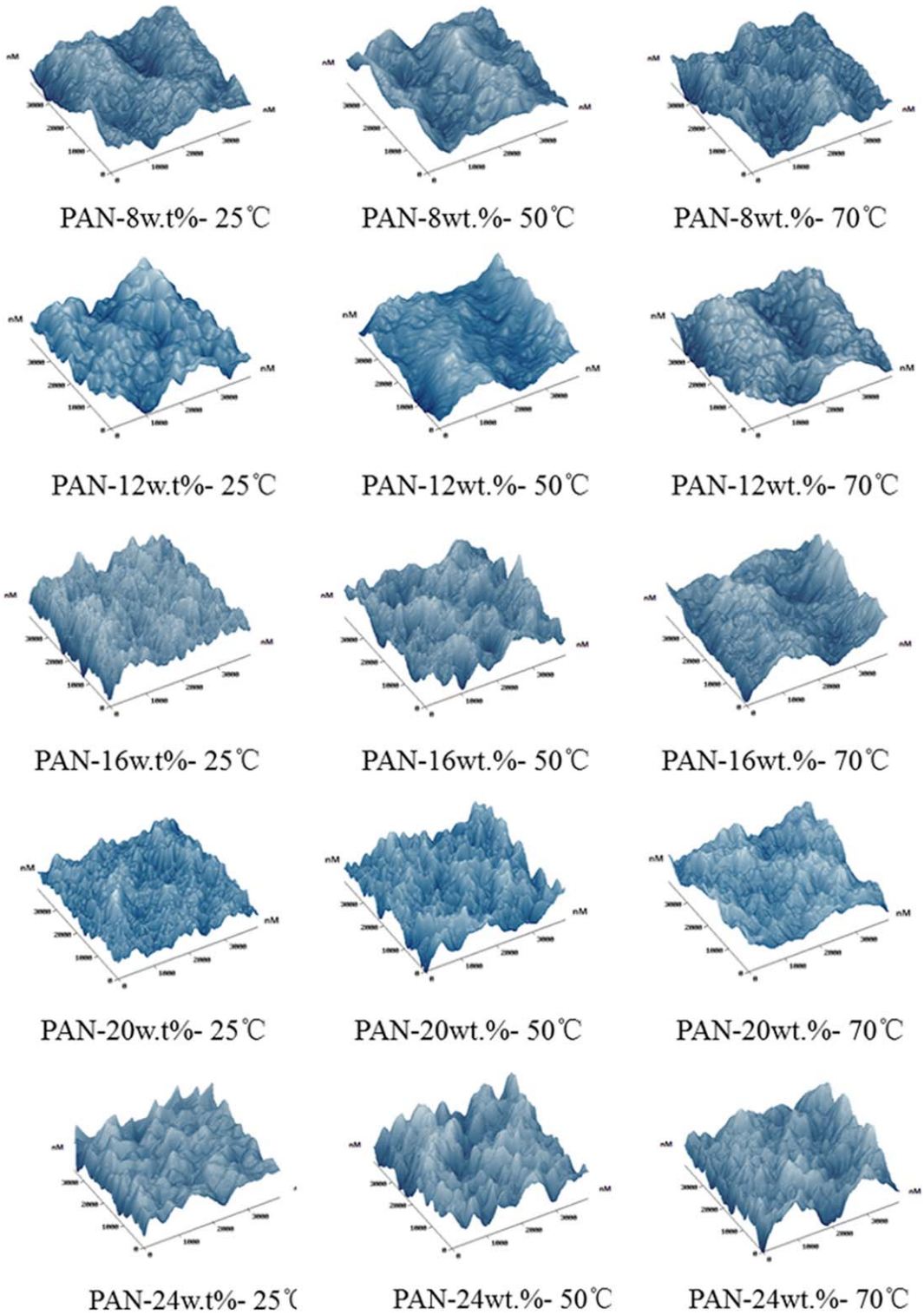

Figure 7. Analysis of AFM images of the PAN membranes. [Color figure can be viewed in the online issue, which is available at wileyonlinelibrary.com.]

by viscosity, polymer dilute solutions with different concentrations were prepared for probing the flowing time of solution at 25°C. The results were shown in Figure 2. According to the results, the inherent viscosity can be obtained by the extrapolation method. Theoretically, the two straight lines should cross into one point on the y axis. Therefore, the obtained viscosity average molecular weight of PAN is 5.8×10^4 g/mol.

Phase Diagrams

Figure 3 shows the experimental cloud-point data for H_2O/DMF/PAN and H_2O/DMSO/PAN systems at room temperature. The

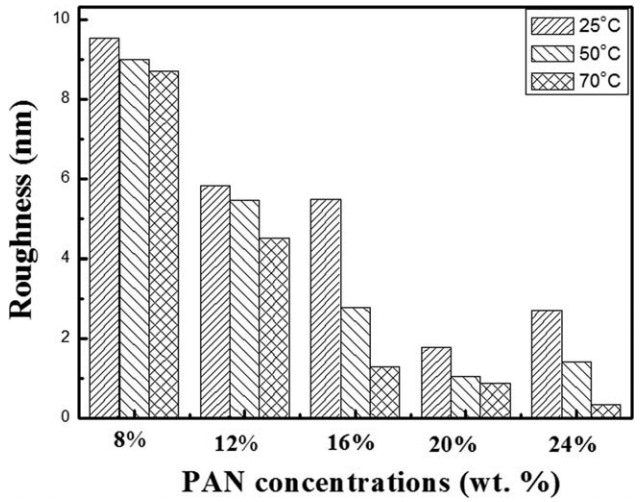

Figure 8. The average surface roughness of PAN membranes fabricated at the different PAN concentrations and coagulant bath temperatures.

comparison between H_2O/DMF/PAN and H_2O/DMSO/PAN reveals that DMSO is the better solvent for dissolving PAN than DMF. Therefore, DMSO is chosen as the typical solvent for the further study. To explore the temperature effects on PAN solubility, the cloud-point curves of H_2O/DMSO/PAN system at 50°C and 70°C have been demonstrated in Figure 4. According to Figure 4, the solubility is slightly better at higher temperature possibly due to the enhanced polymer–solvent interactions.

Pure Water Flux and BSA Rejection

The results of pure water flux and BSA rejection are listed in Table I. The water flux of PAN membrane fabricated at the lower PAN concentration is much larger than that fabricated at the higher PAN concentration. It indicates that porosity of PAN membranes fabricated at the lower polymer concentration is larger. These results are consistent with the results of the cross-section morphology examination of the membranes by SEM. All membranes can achieve a high level of BSA rejection (100%). Compared to other reported results,[39,40] the developed membrane in this study demonstrate the better comprehensive performance with both higher flux and rejection. For example, the membrane fabricated with 16 wt % PAN solution has the high flux reaching 213.8 L/m/bar with the BSA rejection of 100%. However, when concentration of PAN was 8 wt % and 12 wt %, the mechanical strength of membranes is too low to determine the water flux of the membrane, which is due to the highly developed pore structure existing in the membranes. Therefore, the water flux and BSA rejection cannot be measured. Besides the high porosity of the membranes, the hydrophilicity and the pore microstructure may also contribute to the higher flux and BSA rejection fabricated at the lower polymer concentration and higher temperature. However, the hydrophilicity and the pore microstructure seem to have the less effect on the separation performance of membranes when comparing to the porosity in this study.

Membrane Morphology

Figure 5 illustrates the top surface morphology of membranes prepared by H_2O/DMSO/PAN ternary system. The pores can be observed clearly in Figure 5. When increasing the polymer concentration, the amount of pores on membranes decreases. The very large pores exist on the surface of membrane fabricated at the PAN concentration of 8 wt %. However, there are no such large pores observed on PAN membranes prepared by PAN concentrations of 12 wt %, 16 wt %, 20 wt %, and 24 wt %. Figure 6 shows the cross-section morphologies of membrane developed at different PAN concentration and various temperatures. The comparison of cross-section morphologies of membranes fabricated at different concentrations indicates that the pores in membranes prepared at the lower polymer concentration have channel-like structures with open ends. It is well known that spinodal separation and nucleation/growth separation are the two kinds of separation for membrane formation during phase inversion. Such membranes formed at the lower polymer concentration are almost typical membranes formed by spinodal separation.[41] It can also be explained that the viscosity of system increases when increasing the polymer concentration, reducing the exchange rate of non-solvent and solvent at the phase separation stage. There are other reports[36,42–46] demonstrating that the non-solvent and solvent exchange rate is the most important factors in determining the final structure of membranes. The structure changes from channel-like to finger-like, tear-like, and sponge-like with increasing of polymer concentration. During the phase separation process, the homogeneous polymer solution is separated into two phases: a solid, polymer-rich phase that forms the matrix of the membranes and a liquid, polymer-lean phase that forms the membrane pores.[47] Besides, viscosity of casting solution, temperature of polymer solution and coagulation bath can also affect the exchange rate and the final structure.[48–51] The tendency of morphological evolution of membranes fabricated by varying polymer concentrations at the higher temperature is similar to that at room temperature. When comparing the structures of membranes prepared at the same polymer concentration under different temperatures, it can be confirmed that the pores formed at the higher temperature are looser.

AFM images of PAN membranes are illustrated in Figure 7 and the average surface roughness of various membranes are

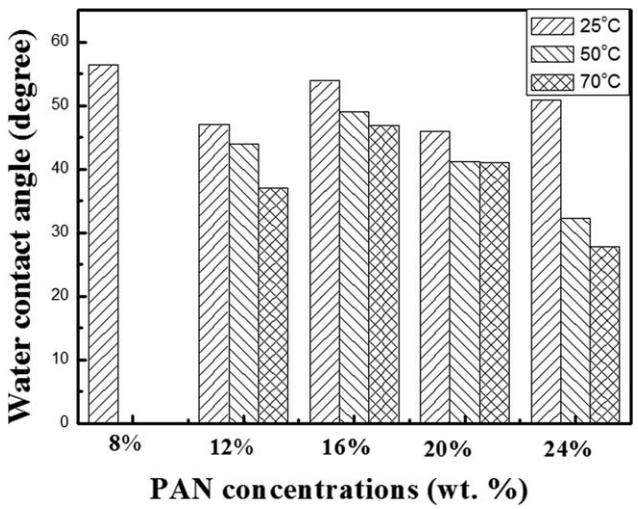

Figure 9. Water contact angles of PAN membranes fabricated at the different PAN concentrations and coagulant bath temperatures.

Table II. Contact Angles and Surface Tension of Different UF Membranes Fabricated by Various Concentrations of PAN in DMSO

PAN concentrations (wt %)	Temperatures (^{O}C)	Contact angle (degree)		γ^{d} (mJ/m^2)	γ^{p} (mJ/m^2)
		water	glycol		
8	25	56.5	22.6	21.2	24.0
	50	-	3.7	-	-
	70	-	-	-	-
12	25	47	21.4	12.5	39.2
	50	44	14.1	12.8	41.2
	70	37	13.2	8.5	52.7
16	25	53.9	24.7	17.1	29.1
	50	49.1	12.3	17.8	32.2
	70	46.9	10. 7	16.1	35.4
20	25	46	27.5	9.1	44.5
	50	41.2	16.6	10.1	47.0
	70	41	20.9	8.6	49.4
24	25	50.9	17.1	17.8	30.8
	50	32.2	14.3	6.1	60.9
	70	27.8	13.8	4.6	67.3

demonstrated in Figure 8. According to Figures 7 and 8, membranes surfaces become smoother when increasing the polymer concentration and coagulation bath temperature. In addition, the larger pores of membranes formed at the lower polymer concentration may contribute to the surface roughness as well.

Hydrophilicity

Figure 9 shows the water contact angle results of PAN membranes. The membrane formed at the 8 wt % polymer concentration and 25°C coagulation bath temperature has the largest contact angle. The contact angles of membranes formed at the same polymer concentration decrease with the temperatures. With the membranes fabricated at 24 wt % polymer concentration as the examples, the contact angle decreases about 20 degrees when the coagulation bath temperature decreases from 50 to 70°C. On the other hand, the contact angles of membranes fabricated at the same temperature decrease with increasing the polymer concentration. When the polymer concentration is 8 wt % and the coagulation bath temperature is 50°C or 70°C, the water is immediately absorbed by the membranes after dropping on the membrane because of the extremely developed pore structures under such conditions.

To improve the hydrophilicity of membrane for enhancing the anti-fouling performance, the most commonly used strategy is to introduce hydrophilic structure in polymer materials or to graft hydrophilic groups on the membrane surface.[28–32] There is seldom report about the influence of different polymer concentrations and coagulation bath temperatures on the membrane hydrophilicity. This study indicates that the effects of different polymer concentrations and coagulation bath temperatures on the membrane hydrophilicity cannot be ignored. This may be due to the possible relationship between the hydrophilicity of membranes and the pore structure or surface roughness.[52,53]Besides, to confirm the relationship of the hydrophilicity and surface tension of membranes, glycol contact angles of membranes are also measured and the results are demonstrated in Table II. The decline of water contact angles indicates that the surfaces of membranes fabricated at the higher temperatures are much polar. Generally, the polarity of a surface can be quantitatively characterized by the polar component (γ^{p}) of the surface tension. The changing of polar component of the membranes may be due to the changing of micro structure of the membranes by adjusting the phase inversion conditions, which will be investigated in our future work.

CONCLUSIONS

The phase diagram proves that DMSO is a better solvent than DMF for dissolving PAN. The basic performance of membrane fabricated at 16 wt % PAN concentration (in DMSO) and 25°C is excellent with the water flux of 213.8 L/m/bar and BSA rejection of 100%. The membrane structures examined by SEM develop from channel-like to tear-like and further to sponge-like structures when increasing the polymer concentration because of the different separating routes. Higher temperature of coagulation bath produces the pores with the much looser structure which is due to the increased exchanging rate between non-solvent and solvent. Roughness of the membrane surface reduces and the membrane surface becomes smoother when increasing the polymer concentration and coagulation bath temperature. The hydrophilicity of membranes improves with increasing the PAN concentration and temperature of coagulation bath.

ACKNOWLEDGMENTS

This work was supported by National Natural Science Foundation of China (21177032, U1462103), Program for New Century

Excellent Talents in University (NCET-11–0805), the Fundamental Research Funds for the Central Universities (Grant No. HIT.BRETIV.201307), Harbin Science and Technology Innovation Talent Funds (2014RFXXJ028), and State Key Laboratory of Urban Water Resource and Environment (Harbin Institute Technology) (No. 2014DX05).

REFERENCES

1. Strathman, H. Proceedings of International Congress on Membrane and Membrane Progress [C]. (ICOM90 Chicago USA) **1990**, *1*, 1167–1168.
2. Cot, L. Proccedings of the Third International Comference on Inorgnic Membrance [M]. Worcoster USA, **1994**, *157*.
3. Shi, D. Q.; Kong, Y.; Yu, J. X.; Wang, Y. F.; Yang, J. R. *Desalination* **2006**, *196*, 309.
4. Jiang, L. Y.; Wang, Y.; Chung, T. S.; Qiao, X. Y.; Lai, J. Y. *Prog. Polym. Sci.* **2009**, *34*, 1135.
5. Shao, L.; Cheng, X. Q.; Liu, Y.; Quan, S.; Ma, J.; Zhao, S. Z.; Wang, K. Y. *J. Membr. Sci.* **2013**, *430*, 96.
6. Cheng, X. Q.; Shao, L.; Lau, C. H. *J. Membr. Sci.* **2015**, *476*, 95.
7. Jiang, L. Y.; Chung, T. S.; Cao, C.; Huang, Z.; Kulprathipanja, S. *J. Membr. Sci.* **2005**, *252*, 89.
8. Xing, D. Y.; Chan, S. Y.; Chung, T. S. *Green Chem.* **2014**, *16*, 1383.
9. Sorribas, S.; Gorgojo, P.; Te´llez, C.; Coronas, J.; Livingston, A. G. *J. Am. Chem. Soc.* **2013**, *135*, 15201.
10. Gorgojo, P.; Karan, S.; Wong, H. C.; Jimenez-Solomon, M. F.; Cabral, J. T.; Livingston, A. G. *Adv. Funct. Mater.* **2014**, *24*, 4729.
11. Marchetti, P.; Jimenez Solomon, M. F.; Szekely, G.; Livingston, A. G. *Chem. Rev.* **2014**, *114*, 10735.
12. Wang, Z. X.; Lau, C. H.; Zhang, N. Q.; Bai, Y. P.; Shao, L. *J. Mater. Chem. A* **2015**, *3*, 2650.
13. Mulder, M. Basic Principles of Membrane Technology. Kluwer Academic Publishers: Dordrecht, **1996**.
14. Baker, R. W. Membrane Technology and Applications, 2nd edition. John Wiley & Sons Ltd.: England, **2004**.
15. Yilmaz, L.; McHugh, A. *J. Appl. Polym. Sci.* **1986**, *31*, 997.
16. Zeman, L.; Tkacik, G. *J. Membr. Sci.* **1988**, *36*, 119.
17. Kim, J. Y.; Lee, H. K.; Baik, K. J. *J. Appl. Polym. Sci.* **1997**, *65*, 2643.
18. Zhang, J.; Zhang, Y. W.; Zhao, J. X. *Polym. Bull.* **2011**, *67*, 1073.
19. Kang, J. S.; Lee, Y. M. *J. Appl. Polym. Sci.* **2002**, *85*, 57.
20. Tan, L. A.; Pan, D.; Pan, N. *J. Appl. Polym. Sci.* **2008**, *110*, 3439.
21. Madaeni, S. S.; Bakhtiari, L. *Polymer* **2012**, *53*, 4481.
22. Chung, T. S. *J. Membr. Sci.* **1997**, *126*, 19.
23. Li, D. F.; Chung, T. S.; Ren, J. Z.; Wang, R. *Ind. Eng. Chem. Res.* **2004**, *43*, 1553.
24. Widjojo, N.; Chung, T. S. *Ind. Eng. Chem. Res.* **2006**, *45*, 7618.
25. Marshall, A. D.; Munro, P. A.; Traegard, G. *Desalination* **1993**, *91*, 65.
26. Allmer, K.; Hult, A.; Ranby, B. *J. Polym. Sci. Part A: Polym. Chem.* **1988**, *26*, 2099.
27. Hvid, K. B.; Nielsen, P. S.; Stengaard, F. F. *J. Membr. Sci.* **1990**, *53*, 189.
28. Godjevargova, T.; Vonsulov, V.; Dimov, A. *J. Membr. Sci.* **2000**, *172*, 279.
29. Mathias, U.; Georges, B. *J. Membr. Sci.* **1996**, *111*, 193.
30. Mathias, U.; Heike, M.; Annett, O.; Hans-Georg, H. *J. Membr. Sci.* **1996**, *115*, 31.
31. Chen, L.; Shen, X. *Membr. Sci. Technol.* **1997**, *17*, 1.
32. Shao, L.; Wang, Z. X.; Zhang, Y. L.; Jiang, Z. X.; Liu, Y. Y. *J. Membr. Sci.* **2014**, *461*, 10.
33. Cheng, X. Q.; Shao, L.; Lau, C. H. *J. Membr. Sci.* **2015**, *476*, 95.
34. Shao, L.; Cheng, X. Q.; Wang, Z. X.; Ma, J.; Guo, Z. H. *J. Membr. Sci.* **2014**, *452*, 82.
35. Strathmann, H.; Koch, K.; Amar, P.; Baker, R. W. *Desalination* **1975**, *16*, 179.
36. Tan, L. J.; Liu, S. P.; Pan, D. *Colloids. Surf. A* **2009**, *340*, 168.
37. Dong, R. J.; Zhao, J. X.; Zhang, Y. W.; Pan, D. *J. Polym. Sci. Part B: Polym. Phys.* **2009**, *47*, 261.
38. Barzin, J.; Sadatnia, B. *Polymer* **2007**, *48*, 1620.
39. Qin, J. J.; Cao, Y. M.; Li, Y. Q.; Li, Y.; Oo, M. H.; Lee, H. *Sep. Purif. Technol.* **2004**, *36*, 149.
40. Majeed, S.; Fierro, D.; Buhr, Q.; Wing, J.; Du, B.; Boschetti-de-Fierro, A.; Abetz, V. *J. Membr. Sci.* **2012**, 403-404, 101.
41. Barth, C.; Goncalves, M. C.; Pires, A. T. N.; Roeder, J.; Wolf, B. A. *J. Membr. Sci.* **2000**, *169*, 287.
42. Cheng, L. P.; Young, T. H.; Chuang, W. Y.; Chen, L. Y.; Chen, L. W. *Polymer* **2001**, *42*, 443.
43. Altena, F. W.; Smolders, C. A. *Macromolecules* **1982**, *15*, 1491.
44. Barton, B. F.; Mchuge, A. J. *J. Polym. Sci. Part B: Polym. Phys.* **1999**, *37*, 1449.
45. Young, T. H.; Huang, Y. H.; Huang, Y. *Sh. J. Membr. Sci.* **2000**, *171*, 197.
46. Barzin, J.; Feng, C.; Khulbe, K. C.; Matsuura, T.; Madaeni, S. S.; Mirzadeh, H. *J. Membr. Sci.* **2004**, *237*, 77.
47. Barzin, J. Sadatnia, B. *J. Membr. Sci.* **2008**, *325*, 92.
48. Barzin, J.; Madaeni, S. S.; Mirzadeh, H.; Mehrabzadeh, M. *J. Appl. Polym. Sci.* **2004**, *92*, 3804.
49. Barzin, J.; Madaeni, S. S.; Mirzadeh, H. *Iran Polym. J.* **2005**, *14*, 353.
50. Peng, N.; Widjojo, N.; Sukitpaneenit, P.; Teoh, M. M.; Lipscomb, G. G.; Chung, T. S.; Lai, J. Y. *Prog. Polym. Sci.* **2012**, *37*, 1401.
51. Peng, N.; Chung, T. S.; Wang, K. Y. *J. Membr. Sci.* **2008**, *318*, 363.
52. Masahide, T.; Georges, B. *Langmuir* **2002**, *18*, 6465.
53. Kamusewitz, H.; Possart, W. *Appl. Phys. A* **2003**, *76*, 899.